Acta Mech 230, 1513–1527 (2019)
https://doi.org/10.1007/s00707-018-2338-5

ORIGINAL PAPER

Alireza Gharahi · Peter Schiavone

Edge dislocation with surface flexural resistance in micropolar materials

Received: 20 August 2018 / Published online: 5 January 2019

Abstract We employ a micropolar surface model, capable of incorporating bending and twisting rigidities, to analyze the fundamental problem of the deformation of a micropolar half-plane containing a single-edge dislocation. The surface model is based on a Kirchhoff–Love micropolar thin shell of separate elasticity perfectly bonded to the surrounding micropolar bulk. Combining micropolar elasticity with a higher-order surface model allows for the incorporation of size effects well known to be essential in, for example, continuum-based modeling of nanostructured materials. The corresponding boundary value problems are solved analytically using Fourier integral transforms. We illustrate our results by constructing the resulting stress distributions for the most general case of a micropolar material with surface stretching, flexural, and micropolar twisting resistance. To verify our results, we show that under appropriate simplifying assumptions, our solutions reduce to the corresponding solutions in the literature from classical elasticity and also to those which employ micropolar elasticity in the absence of surface effects. Finally, we report on the significance of the contribution of the newly incorporated surface and bulk parameters on the overall solution of the micropolar edge dislocation problem.

1 Introduction

The continued development of enhanced continuum-based models is largely in response to the need to accommodate advanced materials which are known to be strongly influenced by their internal structure, for example, nanomaterials whose representative elements exhibit high surface area-to-volume ratios or solids with significant microstructure such as granular or polymeric materials not accommodated by classical continuum theories [1]. With respect to the latter, theories of generalized continua have been developed to address the deficiencies in classical continuum models via the introduction of additional kinematic parameters and associated tensor fields. For example, micromorphic theory [2–4], a particular case of which is micropolar theory, for which Eringen [5,6] defines generalized continuum models as a collection of deformable elements free to move independently in local 'micromotions'. The most general form of micromorphic theory imposes no restrictions on the micromotions, while the subclass of micropolar materials limits the internal motion of elements to rigid rotations around their center of mass [7]. The micropolar theory for solids has been applied to the solution of several fundamental problems of elasticity [8–12].

In the case of nanomaterials in which the predominant factor is high surface area-to-volume ratios, classical continuum models have been enhanced via the incorporation of surface effects using, for example, the well-

A. Gharahi, P. Schiavone (✉)
Department of Mechanical Engineering, University of Alberta, Edmonton, AB T6G 1H9, Canada
E-mail: p.schiavone@ualberta.ca
Tel. 780 492 3638

A. Gharahi
E-mail: gharahi@ualberta.ca

established surface model of Gurtin and Murdoch (G–M) [13,14] which treats the surface as a thin classical elastic membrane with separate elasticity perfectly bonded to the surrounding bulk material. Several applications of the G–M theory can be found, for example [15–19]. Steigmann and Ogden [20,21] subsequently generalized the G–M model to incorporate both stretching and flexural resistance thus providing the stability to the G–M model required to accommodate certain compressive surface stresses (see for example [22]). Although, from its earliest appearance in the literature, the Steigmann–Ogden (S–O) model has attracted the attention of several researchers (see for example, [23,24] which study the linearized version of the S–O model), its incorporation into surface models to account for size dependency in elastic solids is a more recent trend (see, for example, Chhapadia et al. [25] which examines the properties of an elastic surface at the nanoscale when subjected to tension and bending; Chen and Chiu [26] which categorizes the S–O surface model using a classification principle as in [27]; Eremeyev and Lebedev [28] which formulates existence and uniqueness theorems for boundary value problems based on the S–O model; Dai et al. [29] and Zemlyanova and Mogilevskaya [30] which solve the fundamental problem of a circular inhomogeneity with bending resistant interface; and [31–33] which consider fracture and contact problems in the framework of the S–O model).

Since the two aforementioned approaches (i.e., generalized continuum theories and continuum models enhanced with surface theories) each establish a separate gateway to the introduction of size dependency in nanoscaled materials, intuitively, it would seem that their unification into a single model should result in a more comprehensive account of size effects in continuum-based models. However, such studies are rather rare in the literature, perhaps as a result of the complexity of the equations involved. We do note, however, the following recent important contributions to this area: the extension of the G–M model to micropolar elasticity in [34]; the antiplane micropolar model in [35] which incorporates a simplified contribution from surface effects; the antiplane surface model in a couple stress elastic bulk applied to the mode III crack problem [36]. Most recently, the authors [37] have presented a plane micropolar model which incorporates classical bending resistance of the surface together with micropolar twisting rigidity parameters and have used it to solve fundamental problems involving a circular cavity.

In this paper, we adapt the micropolar surface model presented in [37] (again incorporating bending and twisting rigidities of the surface) to analyze the fundamental problem of the deformation of a micropolar half-plane containing a single-edge dislocation. We use Fourier integral transforms to solve the problem analytically. This problem has been analyzed by Intarit et al. [38] for classical elasticity using the G–M surface model. This provides us a good benchmark with which to check our results and illustrate the added contributions from the enhanced model of deformation including the micropolar effects of the bulk and the micropolar twisting and classical bending resistance of the surface.

2 Plane strain micropolar elasticity

A representative material element in micropolar elasticity transmits not only classical force per unit area (stress) but also moment per unit area (couple stress). For consistency, three independent rotational degrees of freedom characterize the kinematics of a micropolar material in addition to the three classical displacements. The extra rotational degrees of freedom are known as 'microrotations' [6]. In this context, we consider a Cartesian system of coordinates denoted by $\{x_i\}_{i=1}^3$ and formalize plane micropolar elasticity such that the x_1 and x_2 axes lie on the corresponding plane of deformation. In plane deformations, the displacement and microrotation vectors take the forms: $\mathbf{u} = (u_1(x_1, x_2), u_2(x_1, x_2), 0)$ and $\boldsymbol{\varphi} = (0, 0, \varphi_3(x_1, x_2))$, respectively, so that the only nonvanishing degrees of freedom, $\{u_1, u_2, \varphi_3\}$, are independent of the out-of-plane axis, x_3. This scenario is also described as the *first* plane problem in the theory of micropolar elasticity [39]. In this case, in the absence of body forces and body moments, the equilibrium equations are written as [39]

$$\sigma_{\alpha\beta,\alpha} = 0, \tag{1}$$

$$\mu_{\alpha 3,\alpha} + \epsilon_{3\alpha\beta}\sigma_{\alpha\beta} = 0, \tag{2}$$

where Greek indices take the values $\{1, 2\}$ and the convention of summation over repeated indices is adopted. The use of a comma before an index α represents the derivative $\partial/\partial x_\alpha$. Here, $\sigma_{\alpha\beta}$ and $\mu_{\alpha 3}$ denote the corresponding Cartesian components of the stress and couple stress tensors, respectively, and $\epsilon_{3\alpha\beta}$ are the Cartesian components of the permutation tensor. The microstrain tensor $\varepsilon_{\alpha\beta}$, and the microtorsion tensor $\kappa_{3\alpha}$ are associated with a given displacement and rotation field in plane micropolar elasticity via the relations

$$\varepsilon_{\alpha\beta} = u_{\beta,\alpha} - \epsilon_{3\alpha\beta}\varphi_3, \tag{3}$$
$$\kappa_{3\alpha} = \varphi_{3,\alpha}. \tag{4}$$

The constitutive relations for a linear homogeneous isotropic micropolar material subjected to plane deformations are given by [39]

$$\sigma_{\alpha\beta} = (\mu+\alpha)\varepsilon_{\alpha\beta} + (\mu-\alpha)\varepsilon_{\beta\alpha} + \lambda\varepsilon_{\gamma\gamma}\delta_{\alpha\beta}, \tag{5}$$
$$\sigma_{33} = \lambda\varepsilon_{\gamma\gamma}, \tag{6}$$
$$\mu_{\alpha 3} = (\gamma+e)\varphi_{3,\alpha}, \tag{7}$$
$$\mu_{3\alpha} = (\gamma-e)\varphi_{3,\alpha}. \tag{8}$$

The parameters μ and λ are the usual Lamé constants from classical elasticity, while α, γ, and e are the additional elastic constants introduced in micropolar elasticity. We rewrite the microstrain components in terms of displacement and rotation using (3–4) and insert the result into the constitutive equations (5–8). Finally, using the resulting expressions for the stress components in the equilibrium equations (1–2), we obtain

$$(\mu+\alpha)\Delta u_1 + (\mu-\alpha+\lambda)\frac{\partial^2 u_1}{\partial x_1^2} + (\mu-\alpha+\lambda)\frac{\partial^2 u_2}{\partial x_1 \partial x_2} + 2\alpha\frac{\partial}{\partial x_2}\varphi_3 = 0, \tag{9}$$
$$(\mu-\alpha+\lambda)\frac{\partial^2 u_1}{\partial x_1 \partial x_2} + (\mu+\alpha)\Delta u_2 + (\mu-\alpha+\lambda)\frac{\partial^2 u_2}{\partial x_2^2} - 2\alpha\frac{\partial \varphi_3}{\partial x_1} = 0, \tag{10}$$
$$-2\alpha\frac{\partial u_1}{\partial x_2} + 2\alpha\frac{\partial u_2}{\partial x_1} + (\gamma+e)\Delta\varphi_3 - 4\alpha\varphi_3 = 0, \tag{11}$$

where $\Delta \equiv \frac{\partial^2}{\partial x_1^2} + \frac{\partial^2}{\partial x_2^2}$ is the two-dimensional Laplacian. The set of equations (9–11) is a system of three coupled partial differential equations in the three kinematic components (two displacements and one rotation). In the next section, we will complete the mathematical model by introducing appropriate boundary conditions capable of incorporating elastic surface effects. First, however, we decouple the system (9–11) by decomposing the displacement field into potential (gradient) and solenoidal (curl) parts:

$$\mathbf{u} = \nabla \times \boldsymbol{\Psi} + \nabla\Phi, \tag{12}$$

where $\boldsymbol{\Psi}(x_1, x_2)$ and $\Phi(x_1, x_2)$ are, respectively, vector and scalar functions to be determined. The displacement components in plane micropolar deformation therefore become

$$u_1 = \Phi_{,1} + \Psi_{3,2}, \tag{13}$$
$$u_2 = \Phi_{,2} + \Psi_{3,1}. \tag{14}$$

We may write the stress and couple stress components in terms of the functions Φ and Ψ_3:

$$\begin{aligned}
\sigma_{11} &= (2\mu+\lambda)\Delta\Phi + 2\mu\left(\Psi_{3,12} - \Phi_{,22}\right),\\
\sigma_{11} &= (2\mu+\lambda)\Delta\Phi - 2\mu\left(\Psi_{3,12} + \Phi_{,11}\right),\\
\sigma_{12} &= \mu\left(2\Phi_{,12} + \Psi_{3,22} - \Psi_{3,11}\right) - \alpha\Delta\Psi_3 - 2\alpha\varphi_3,\\
\sigma_{21} &= \mu\left(2\Phi_{,12} + \Psi_{3,22} - \Psi_{3,11}\right) + \alpha\Delta\Psi_3 + 2\alpha\varphi_3,\\
\mu_{13} &= (\gamma+e)\varphi_{3,1},\ \ \mu_{23} = (\gamma+e)\varphi_{3,2},\\
\mu_{31} &= (\gamma-e)\varphi_{3,1},\ \ \mu_{32} = (\gamma-e)\varphi_{3,2}.
\end{aligned} \tag{15}$$

Inserting Eqs. (15) into (1–2), we arrive at:

$$(\Delta\Phi)_{,1} + \frac{2\mu}{2\mu+\lambda}\left(c^2\Delta - 1\right)\varphi_{3,2} = 0, \tag{16}$$
$$(\Delta\Phi)_{,2} - \frac{2\mu}{2\mu+\lambda}\left(c^2\Delta - 1\right)\varphi_{3,1} = 0, \tag{17}$$
$$(d^2\Delta - 2)\varphi_3 - \Delta\Psi_3 = 0, \tag{18}$$

where

$$d^2 = \frac{(\gamma + e)}{2\alpha}, \quad c^2 = \frac{(\gamma + e)(\mu + \alpha)}{4\mu\alpha}. \tag{19}$$

The constants d and c (of dimension length) are known as the characteristic lengths of the micropolar material characterizing, in some sense, the micropolar properties of the solid. We combine derivatives of the two equations (16) and (17) to obtain

$$\Delta\Delta\Phi = 0, \tag{20}$$

$$\Delta\left(c^2\Delta - 1\right)\varphi_3 = 0. \tag{21}$$

Each of these equations contains four integration constants to be determined from the boundary conditions and two relations in the form of Cauchy–Riemann equations. In order to obtain the complete solution of the problem, we solve Eqs. (20) and (21) for Φ and φ_3 and carry the resulting φ_3 into Eq. (18) to find the particular solution Ψ_3 of the inhomogeneous equation.

3 Plane micropolar surface model with bending and twisting rigidity

To describe the boundary conditions, we present a surface model that incorporates classical and micropolar bending and twisting rigidities. Let $\mathbf{x}(s^{(1)}, s^{(3)})$ denote the position vector function which associates an ordered pair of real parameters $(s^{(1)}, s^{(3)})$ to a set of points $\mathbf{x}$ in M that form a surface in Euclidean space $\mathbb{R}^3$. We assume that the function $\mathbf{x}(s^{(1)}, s^{(3)})$ is continuously differentiable with respect to each parameter and each point $\mathbf{x}$ of the set M corresponds to a unique pair $(s^{(1)}, s^{(3)})$. In this general context, the tangent and unit normal vectors to the surface are defined as

$$\mathbf{x}_1 = \frac{\partial \mathbf{x}}{\partial s^{(1)}}, \quad \mathbf{x}_3 = \frac{\partial \mathbf{x}}{\partial s^{(3)}}, \quad \mathbf{n} = \frac{\mathbf{x}_1 \times \mathbf{x}_3}{|\mathbf{x}_1 \times \mathbf{x}_3|}. \tag{22}$$

For the surface model in the particular case of plane strain deformations, let $\mathbf{x}_1(s^{(1)}, s^{(3)}) \equiv \mathbf{e}_1(s^{(1)})$ be the unit vector tangent to the surface in the plane of deformation, $\mathbf{x}_3(s^{(1)}, s^{(3)}) \equiv \mathbf{e}_3 =$ constant the unit vector tangent to the surface in the antiplane direction and $\mathbf{n}(s^{(1)}, s^{(3)}) \equiv \mathbf{n}(s^{(1)})$ the unit normal to the surface. In what follows, we replace $s^{(1)}$ by s simply for convenience. We adopt the system of normal-tangential $(n - t)$ coordinates $\{\mathbf{e}_1, \mathbf{e}_3, \mathbf{n}\}$ with respect to which, we define: the surface unit tensor, $\mathbf{I}_\mathrm{s} \equiv \mathbf{I} - \mathbf{n} \otimes \mathbf{n}$, where $\mathbf{I}$ is the second-order unit tensor and $\otimes$ denotes the tensor product of two vectors: the gradient operator, $\nabla \equiv \nabla_\mathrm{s} + \mathbf{n}\frac{\partial(\cdot)}{\partial z}$ when applied to a scalar function; the gradient operator, $\nabla \equiv \nabla_\mathrm{s} + \frac{\partial(\cdot)}{\partial z} \otimes \mathbf{n}$ when applied to a vector function; the surface gradient when applied to a scalar function, $\nabla_\mathrm{s} w \equiv \frac{\partial w}{\partial s}\mathbf{e}_1(s)$; the surface gradient when applied to a vector function, $\nabla_\mathrm{s}\mathbf{u} \equiv \frac{\partial \mathbf{u}}{\partial s} \otimes \mathbf{e}_1(s)$; and the curvature tensor $\mathbf{B} \equiv -\nabla_\mathrm{s}\mathbf{n} = b_{11}\mathbf{e} \otimes \mathbf{e}_1$. Geometrically, the curvature component b_{11} is equivalent to $-\frac{1}{R(s)}$, for $R(s)$ the radius of curvature. We describe the surface as a thin elastic micropolar shell of Kirchhoff–Love type which incorporates bending and twisting resistance. A schematic of the micropolar shell and the adopted normal and tangential coordinates is shown in Fig. 1.

Let the set of points $\mathbf{r}$, satisfying the relation

$$\mathbf{r}(s^{(1)}, s^{(3)}) = \mathbf{x}(s^{(1)}, s^{(3)}) + z\mathbf{n}(s^{(1)}), \quad -\frac{t}{2} \le z \le \frac{t}{2}, \tag{23}$$

define a micropolar shell reinforcing the boundary or the interface of a plane micropolar structure. Then, we may write

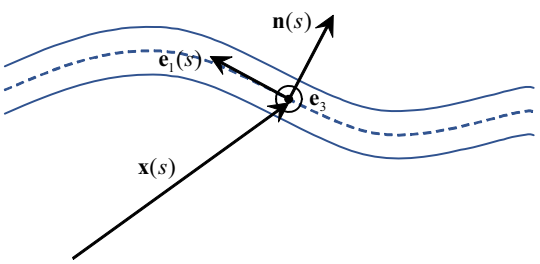

Fig. 1 The configuration of a surface as a shell in plane deformation

$$\mathbf{r}_1 = \frac{\partial \mathbf{r}}{\partial s^{(1)}} = \mathbf{x}_1 + z\frac{\mathrm{d}\mathbf{n}}{\mathrm{d}s} = (\mathbf{I} - z\mathbf{B})\mathbf{e}_1, \tag{24}$$

$$\mathbf{r}_3 = \mathbf{x}_3 + z\frac{\mathrm{d}\mathbf{n}}{\mathrm{d}s^{(3)}} = \mathbf{e}_3, \quad -\frac{t}{2} \le z \le \frac{t}{2}. \tag{25}$$

We define independent displacement and microrotation fields in the micropolar shell in accordance with the following hypothesis: (1) The tangential displacements vary linearly within the shell's thickness. (2) The normal component of displacement as well as the microrotation remains constant across the shell's thickness. Therefore, we may write

$$\mathbf{u} = \mathbf{u}_0(s) - z\mathbf{v}_0(s) + u_n(s)\mathbf{n}, \tag{26}$$

$$\boldsymbol{\varphi} = \boldsymbol{\varphi}_0(s) + \varphi_n(s)\mathbf{n} = \varphi_3(s)\mathbf{e}_3, \tag{27}$$

where $\mathbf{u}_0$ is the tangential displacement of the median surface of the shell, u_n is the normal component of the displacement, $\boldsymbol{\varphi}_0$ is the tangential microrotation, and φ_n is the normal component of the microrotation. It is not difficult to see that for the first problem of micropolar plane strain, φ_3 remains the only nonvanishing component of the microrotation vector. Using the definitions of the gradient operator above and Eq. (26), we obtain

$$(\nabla\mathbf{u})^{\mathrm{T}} = (\nabla_{\mathrm{s}}\mathbf{u}_0)^{\mathrm{T}} - z(\nabla_{\mathrm{s}}\mathbf{v}_0)^{\mathrm{T}} - (\mathbf{n}\otimes\mathbf{v}_0) + (\nabla u_n \otimes \mathbf{n}) - u_n\mathbf{B}, \tag{28}$$

where the superscripts T indicate the transpose of a tensor. Additionally, we define the permutation vector of the microrotation in this particular plane strain condition as:

$$\boldsymbol{\varphi}_\times = \varphi_3(\mathbf{n}\otimes\mathbf{e}_1) - \varphi_3(\mathbf{e}_1\otimes\mathbf{n}). \tag{29}$$

The surface microstrain tensor is defined as:

$$\boldsymbol{\varepsilon}^s = (\nabla\mathbf{u})^{\mathrm{T}} - \boldsymbol{\varphi}_\times. \tag{30}$$

We expand Eq. (30) using (28) and (29) and note the following:

$$\begin{aligned}
\frac{\mathrm{d}\mathbf{e}_1}{\mathrm{d}s} &= b_{11}\mathbf{n},\\
\mathbf{u}_0 &= u_0(s)\mathbf{e}_1(s), \quad \mathbf{v}_0 = v_0(s)\mathbf{e}_1(s),\\
(\nabla_{\mathrm{s}}\mathbf{u}_0)^{\mathrm{T}} &= \frac{\mathrm{d}u_0}{\mathrm{d}s}(\mathbf{e}_1\otimes\mathbf{e}_1) + b_{11}u_0(\mathbf{e}_1\otimes\mathbf{n}),\\
(\nabla_{\mathrm{s}}\mathbf{v}_0)^{\mathrm{T}} &= \frac{\mathrm{d}v_0}{\mathrm{d}s}(\mathbf{e}_1\otimes\mathbf{e}_1) + b_{11}v_0(\mathbf{e}_1\otimes\mathbf{n}),\\
\nabla u_n &= \nabla_{\mathrm{s}}u_n = \frac{\mathrm{d}u_n}{\mathrm{d}s}\mathbf{e}_1.
\end{aligned} \tag{31}$$

We add to these the assumption of a sufficiently thin and smooth shell such that terms $t\,\|\mathbf{B}\| \ll 1$ ($\|\cdot\|$ denotes the norm of the tensor defined as usual by $\|\mathbf{A}\| = (\mathbf{A}:\mathbf{A})^{1/2}$) so that any term of the form $z\mathbf{B}$ becomes negligible. The surface microstrain tensor is now expressed as:

$$\begin{aligned}
\boldsymbol{\varepsilon}^s = &\left(\frac{\mathrm{d}u_0}{\mathrm{d}s} - z\frac{\mathrm{d}v_0}{\mathrm{d}s} - u_n b_{11}\right)(\mathbf{e}_1\otimes\mathbf{e}_1)\\
&+ \left(b_{11}u_0 + \frac{\mathrm{d}u_n}{\mathrm{d}s} + \varphi_3\right)(\mathbf{e}_1\otimes\mathbf{n})\\
&+ (-v_0 - \varphi_3)\,(\mathbf{n}\otimes\mathbf{e}_1)\,.
\end{aligned} \tag{32}$$

The stress–microstrain and couple stress–microrotation relations on a micropolar surface are given as:

$$\boldsymbol{\sigma}^s = (\mu_{\mathrm{s}} + \alpha_{\mathrm{s}})\varepsilon^s + (\mu_{\mathrm{s}} - \alpha_{\mathrm{s}})\varepsilon^{s\mathrm{T}} + \lambda_{\mathrm{s}}(\mathrm{tr}\,\boldsymbol{\varepsilon}^s)\mathbf{I}_{\mathrm{s}}, \tag{33}$$

$$\boldsymbol{\mu}^s = (\gamma_{\mathrm{s}} + \epsilon_{\mathrm{s}})(\nabla\boldsymbol{\varphi})^{\mathrm{T}} + (\gamma_{\mathrm{s}} - \epsilon_{\mathrm{s}})\nabla\boldsymbol{\varphi} + \beta_{\mathrm{s}}(\mathrm{div}\,\boldsymbol{\varphi})\mathbf{I}_{\mathrm{s}}, \tag{34}$$

where μ_s, α_s, λ_s, γ_s, ϵ_s and β_s are surface elastic constants. We substitute the expressions from Eqs. (32) and (27) for $\boldsymbol{\varepsilon}^s$ and $\boldsymbol{\varphi}$, to obtain:

$$\begin{aligned}\boldsymbol{\sigma}^s = &(2\mu_s+\lambda_s)\left(\frac{\mathrm{d}u_0}{\mathrm{d}s}-z\frac{\mathrm{d}v_0}{\mathrm{d}s}-u_n b_{11}\right)(\mathbf{e}_1\otimes\mathbf{e}_1)\\ &+\left[\mu_s\left(\frac{\mathrm{d}u_n}{\mathrm{d}s}+b_{11}u_0-v_0\right)+\alpha_s\left(\frac{\mathrm{d}u_n}{\mathrm{d}s}+b_{11}u_0+v_0+2\varphi_2\right)\right](\mathbf{e}_1\otimes\mathbf{n})\\ &+\left[\mu_s\left(\frac{\mathrm{d}u_n}{\mathrm{d}s}+b_{11}u_0-v_0\right)-\alpha_s\left(\frac{\mathrm{d}u_n}{\mathrm{d}s}+b_{11}u_0+v_0+2\varphi_2\right)\right](\mathbf{n}\otimes\mathbf{e}_1)\\ &+\lambda_s\left(\frac{\mathrm{d}u_0}{\mathrm{d}s}-z\frac{\mathrm{d}v_0}{\mathrm{d}s}-u_n b_{11}\right)(\mathbf{e}_3\otimes\mathbf{e}_3),\end{aligned}\tag{35}$$

$$\boldsymbol{\mu}^s=(\gamma_s+e_s)\frac{\mathrm{d}\varphi_3}{\mathrm{d}s}(\mathbf{e}_1\otimes\mathbf{e}_3)+(\gamma_s-e_s)\frac{\mathrm{d}\varphi_3}{\mathrm{d}s}(\mathbf{e}_3\otimes\mathbf{e}_1).\tag{36}$$

We denote by $f_1^+(s)$ and $f_1^-(s)$, the tangential component of the force traction vector on the outer (+) and inner (−) faces of the shell (with respect to the positive sense of the unit outward normal vector to the surface). Likewise, we denote the normal component of the force traction vector on the outer/inner (+/−) faces by $f_n^+(s)$ and $f_n^-(s)$, and the couple traction vector on the outer/inner (+/−) faces by $m_3^+(s)$ and $m_3^-(s)$. The equilibrium equations for a thin micropolar shell in $n-t$ coordinates can be written as:

$$\frac{\mathrm{d}\sigma_{11}^s}{\mathrm{d}s}-\sigma_{1n}^s b_{11}=0,\tag{37}$$

$$\frac{\mathrm{d}\sigma_{1n}^s}{\mathrm{d}s}+\sigma_{11}^s b_{11}=0,\tag{38}$$

$$\frac{\mathrm{d}\mu_{13}^s}{\mathrm{d}s}-(\sigma_{1n}^s-\sigma_{n1}^s)=0.\tag{39}$$

We integrate Eqs. (37)–(39) over the thickness, $z\in\left[-\frac{t}{2},\frac{t}{2}\right]$, while including the traction on the faces of the shell and exchanging the components by their expressions from Eqs. (35) and (36). This leads us to the three equilibrium equations:

$$\begin{aligned}&A_s\frac{\mathrm{d}}{\mathrm{d}s}\left(\frac{\mathrm{d}u_0}{\mathrm{d}s}-u_n b_{11}\right)-\left[\mu_s t\left(\frac{\mathrm{d}u_n}{\mathrm{d}s}+b_{11}u_0-v_0\right)b_{11}\right.\\ &\left.+\alpha_s t\left(\frac{\mathrm{d}u_n}{\mathrm{d}s}+b_{11}u_0+v_0+2\varphi_3\right)b_{11}\right]+f_1^+-f_1^-=0,\end{aligned}\tag{40}$$

$$\begin{aligned}&A_s\left(\frac{\mathrm{d}u_0}{\mathrm{d}s}-u_n b_{11}\right)b_{11}+\left[\mu_s t\left(\frac{\mathrm{d}^2u_n}{\mathrm{d}s^2}+\frac{\mathrm{d}(b_{11}u_0)}{\mathrm{d}s}-\frac{\mathrm{d}v_0}{\mathrm{d}s}\right)\right.\\ &\left.+\alpha_s t\left(\frac{\mathrm{d}^2u_n}{\mathrm{d}s^2}+\frac{\mathrm{d}(b_{11}u_0)}{\mathrm{d}s}+\frac{\mathrm{d}v_0}{\mathrm{d}s}+2\frac{\mathrm{d}\varphi_3}{\mathrm{d}s}\right)\right]+f_n^+-f_n^-=0,\end{aligned}\tag{41}$$

$$H_s\frac{\mathrm{d}^2\varphi_3}{\mathrm{d}s^2}-2\alpha_s t\left(\frac{\mathrm{d}u_n}{\mathrm{d}s}+b_{11}u_0+v_0+2\varphi_3\right)+m_3^+-m_3^-=0,\tag{42}$$

where from Eqs. (35) and (36) we identify the stretching and the first twisting rigidity of the shell as: $A_s=2\mu_s+\lambda_s$ and $H_s=\gamma_s+e_s$, respectively. To complete the shell model, we take the vector product of the terms of the equilibrium equation with $z\mathbf{n}$ to construct the stress couples equilibrium around the median surface of the shell:

$$z\mathbf{n}\times\frac{\mathrm{d}\boldsymbol{\sigma}_1}{\mathrm{d}s}+z\mathbf{n}\times\frac{\mathrm{d}\boldsymbol{\sigma}_n}{\mathrm{d}z}=\mathbf{0}.\tag{43}$$

Here, $\boldsymbol{\sigma}_1$ and $\boldsymbol{\sigma}_n$ are the stress vectors acting on the surfaces with unit outward normals, $\mathbf{e}_1$ and $\mathbf{n}$, respectively. We rewrite (43) as follows:

$$\frac{\mathrm{d}(z\mathbf{n}\times\sigma_1)}{\mathrm{d}s}-z\frac{\mathrm{d}\mathbf{n}}{\mathrm{d}s}\times\boldsymbol{\sigma}_1+\frac{\mathrm{d}(z\mathbf{n}\times\sigma_n)}{\mathrm{d}z}-\mathbf{n}\times\boldsymbol{\sigma}_n=\mathbf{0}.\tag{44}$$

We employ Eq. (24) to convert (44) to the form

$$\frac{\mathrm{d}(z\mathbf{n}\times\sigma_1)}{\mathrm{d}s}-\mathbf{r}_1\times\boldsymbol{\sigma}_1+\mathbf{e}_1\times\boldsymbol{\sigma}_1+\frac{\mathrm{d}(z\mathbf{n}\times\sigma_n)}{\mathrm{d}z}-\mathbf{n}\times\boldsymbol{\sigma}_n=\mathbf{0}. \tag{45}$$

Here, we adopt the system of coordinates $\{\mathbf{r}_1,\mathbf{r}_3,\mathbf{n}\}$, and write the couple stress equilibrium equation in that system to show that

$$\mathbf{r}_1\times\boldsymbol{\sigma}_1=-\frac{\mathrm{d}\boldsymbol{\mu}_1}{\mathrm{d}s}-\mathbf{n}\times\sigma_n. \tag{46}$$

We use this relation to arrive at

$$\frac{\mathrm{d}(z\mathbf{n}\times\sigma_1)}{\mathrm{d}s}+\frac{\mathrm{d}\boldsymbol{\mu}_1}{\mathrm{d}s}+\mathbf{n}\times\sigma_n+\mathbf{e}_1\times\boldsymbol{\sigma}_1+\frac{\mathrm{d}(z\mathbf{n}\times\sigma_n)}{\mathrm{d}z}-\mathbf{n}\times\boldsymbol{\sigma}_n=\mathbf{0}, \tag{47}$$

or again in our usual $(n-t)$ coordinates, $\{\mathbf{e}_1,\mathbf{e}_3,\mathbf{n}\}$, we write:

$$\left[\frac{\mathrm{d}(z\sigma_{11})}{\mathrm{d}s}+\frac{\mathrm{d}\mu_{13}}{\mathrm{d}s}-\sigma_{1n}\right]\mathbf{e}_2+\frac{\mathrm{d}(z\mathbf{n}\times\sigma_n)}{\mathrm{d}z}=\mathbf{0}. \tag{48}$$

Integrating over the thickness $z\in\left[-\frac{t}{2},\frac{t}{2}\right]$ and using the fact that

$$\int_{-t/2}^{t.2}\frac{\mathrm{d}(z\mathbf{n}\times\sigma_n)}{\mathrm{d}z}\mathrm{d}z=[z\mathbf{n}\times\sigma_n]_{z=-\frac{t}{2}}^{z=\frac{t}{2}}=\frac{t}{2}(f_1^+ + f_1^-)\mathbf{e}_2, \tag{49}$$

we arrive at a fourth governing condition

$$\begin{aligned}&\left[\mu_s t\left(\frac{\mathrm{d}u_n}{\mathrm{d}s}+b_{11}u_0-v_0\right)+\alpha_s t\left(\frac{\mathrm{d}u_n}{\mathrm{d}s}+b_{11}u_0+v_0+2\varphi_3\right)\right]\\&\quad=-B_s\frac{\mathrm{d}^2v_0}{\mathrm{d}s^2}+H_s\frac{\mathrm{d}^2\varphi_3}{\mathrm{d}s^2}+\frac{t}{2}(f_1^+ + f_1^-),\end{aligned} \tag{50}$$

where B_s indicates the classical bending rigidity of the surface. We introduce this condition into the two equations (40) and (41) to obtain the three boundary equations forming the boundary value problem in plane strain micropolar elasticity:

$$A_s\left(\frac{\mathrm{d}^2u_0}{\mathrm{d}s^2}-\frac{\mathrm{d}(u_nb_{11})}{\mathrm{d}s}\right)+B_sb_{11}\frac{\mathrm{d}^2v_0}{\mathrm{d}s^2}-H_sb_{11}\frac{\mathrm{d}^2\varphi_3}{\mathrm{d}s^2}-\frac{tb_{11}}{2}(f_1^+ + f_1^-)+f_1^+ - f_1^- = 0, \tag{51}$$

$$A_s\left(\frac{\mathrm{d}u_0}{\mathrm{d}s}-u_nb_{11}\right)b_{11}-B_s\frac{\mathrm{d}^3v_0}{\mathrm{d}s^3}+H_s\frac{\mathrm{d}^3\varphi_3}{\mathrm{d}s^3}+\frac{t}{2}\left(\frac{\mathrm{d}f_1^+}{\mathrm{d}s}+\frac{\mathrm{d}f_1^-}{\mathrm{d}s}\right)+f_n^+ - f_n^- = 0, \tag{52}$$

$$H_s\frac{\mathrm{d}^2\varphi_3}{\mathrm{d}s^2}-2L_s\left(\frac{\mathrm{d}u_n}{\mathrm{d}s}+b_{11}u_0+v_0+2\varphi_3\right)+m_3^+ - m_3^- = 0, \tag{53}$$

where $L_s=\alpha_s t$ is the second twisting rigidity of the micropolar surface. To further simplify the surface model, we employ the Kirchhoff–Love's kinematic hypothesis to exclude shear deformation effects throughout the surface thickness. This assumption implies that

$$\mathbf{v}_0=\mathbf{B}\mathbf{u}_0+\nabla_s u_n. \tag{54}$$

Therefore, the three boundary equations translate to:

$$A_s\left(\frac{d^2u_0}{ds^2}-\frac{d(u_nb_{11})}{ds}\right)+B_sb_{11}\left(\frac{d^2(b_{11}u_0)}{ds^2}+\frac{d^3u_n}{ds^3}\right)-H_sb_{11}\frac{d^2\varphi_3}{ds^2}$$
$$-\frac{tb_{11}}{2}(f_1^+ + f_1^-)+f_1^+ - f_1^- = 0, \tag{55}$$
$$A_s\left(\frac{du_0}{ds}-u_nb_{11}\right)b_{11}-B_s\left(\frac{d^3(b_{11}u_0)}{ds^3}+\frac{d^4u_n}{ds^4}\right)$$
$$+H_s\frac{d^3\varphi_3}{ds^3}+\frac{t}{2}\left(\frac{df_1^+}{ds}+\frac{df_1^-}{ds}\right)+f_n^+ - f_n^- = 0, \tag{56}$$
$$H_s\frac{d^2\varphi_3}{ds^2}-4L_s\left(\frac{du_n}{ds}+b_{11}u_0+\varphi_3\right)+m_3^+ - m_3^- = 0. \tag{57}$$

The foregoing boundary conditions along with the governing equations of the first-plane problem of micropolar elasticity establish a mathematical model of the boundary value problem which incorporates micropolar surface effects with bending resistance. In the next section, we apply this model to determine the analytical solution for the problem of an edge dislocation in a micropolar elastic half-plane with surface elasticity.

4 An edge dislocation in a half-plane medium

Consider an elastic micropolar half-plane with an edge dislocation located at a depth h below the surface. As shown in the figure the dislocation is oriented such that the slip plane is parallel to the free surface. To formulate the edge dislocation, we divide the half-plane into two regions: region (1) defined as the strip described by $0 \le x_1 \le h$ and region (2) the half-plane where $h < x_1$. We associate the parameters' correspondence to each region by a superscript $i = 1, 2$ as $(..)^{(i)}$. The free surface of the original half-plane has the surface elastic properties described in the previous section. Consequently, the surface is endowed with classical bending and stretching rigidities as well as two micropolar twisting moduli. The free surface is planar, and therefore the radius of curvature $R(s)$ tends to infinity and the curvature tensor component $b_{11} = -1/R$ approaches zero. In addition, we assume that the shear traction coupling term, $\frac{t}{2}(\frac{df_1^+}{ds}+\frac{df_1^-}{ds})$, is negligible in Eq. (56). The straight edge dislocation under consideration is shown in Fig. 2.

With respect to the system of coordinates given in the figure, the variable $s = x_2$. The free surface implies that $f_1^- = f_n^- = m_3^- = 0$, while

$$f_1^+ = \sigma_{12}^{(1)}(0, x_2), \quad f_n^+ = \sigma_{12}^{(1)}(0, x_2), \quad m_3^+ = \mu_{13}^{(1)}(0, x_2). \tag{58}$$

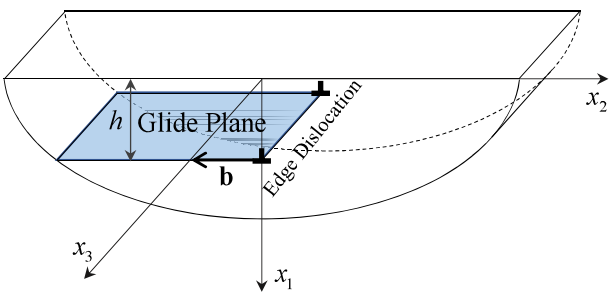

Fig. 2 Edge dislocation in a half-pane with the slip plane parallel to the surface at a depth h

Accordingly, the boundary conditions at the free surface become:

$$A_{\mathrm{s}}\frac{\mathrm{d}^2u_2^{(1)}}{\mathrm{d}x_2^2}\bigg|_{x_1=0}+\sigma_{12}^{(1)}(0,x_2)=0, \tag{59}$$

$$-B_{\mathrm{s}}\frac{\mathrm{d}^4u_1^{(1)}}{\mathrm{d}x_2^4}\bigg|_{x_1=0}+H_{\mathrm{s}}\frac{\mathrm{d}^3\varphi_3^{(1)}}{\mathrm{d}x_2^3}\bigg|_{x_1=0}+\sigma_{11}^{(1)}(0,x_2)=0, \tag{60}$$

$$H_{\mathrm{s}}\frac{\mathrm{d}^2\varphi_3^{(1)}}{\mathrm{d}x_2^2}\bigg|_{x_1=0}-4L_{\mathrm{s}}\left(\varphi_3^{(1)}(0,x_2)+\frac{\mathrm{d}u_1^{(1)}}{\mathrm{d}x_2}\bigg|_{x_1=0}\right)+\mu_{13}^{(1)}(0,x_2)=0. \tag{61}$$

In addition, we have the continuity of displacement, microrotations, stresses and couple stresses along the intersection of the two regions at $x_1=h$. Finally, we characterize the dislocation as a displacement jump across the glide plane ($x_1=h$, $x_2<0$) by the magnitude of a Burgers vector $\mathbf{b}=b\mathbf{e}_2$. Therefore, we have six more boundary conditions to satisfy at $x_1=h$:

$$u_2^{(2)}(h,x_2)-u_2^{(1)}(h,x_2)=bH(-x_2)\equiv F(x_2), \tag{62}$$

$$u_1^{(2)}(h,x_2)=u_1^{(1)}(h,x_2), \tag{63}$$

$$\varphi_3^{(2)}(h,x_2)=\varphi_3^{(1)}(h,x_2) \tag{64}$$

$$\sigma_{11}^{(2)}(h,x_2)=\sigma_{11}^{(1)}(h,x_2), \tag{65}$$

$$\sigma_{12}^{(2)}(h,x_2)=\sigma_{12}^{(1)}(h,x_2), \tag{66}$$

$$\mu_{13}^{(2)}(h,x_2)=\mu_{13}^{(1)}(h,x_2). \tag{67}$$

In Eq. (62), $H(x)$ denotes the Heaviside step function. We solve the three governing equations (18), (20) and (21) for each region using the following Fourier integral transform:

$$\widetilde{f}(x_1,s)=\frac{1}{\sqrt{2\pi}}\int_{-\infty}^{\infty}f(x_1,x_2)e^{-\imath sx_2}\mathrm{d}x_2,$$

$$f(x_1,x_2)=\frac{1}{\sqrt{2\pi}}\int_{-\infty}^{\infty}\widetilde{f}(x_1,s)e^{\imath sx_2}\mathrm{d}x_2, \tag{68}$$

where $\imath=\sqrt{-1}$ is the imaginary unit. The governing equations, consequently, reduce to the ordinary differential equations:

$$\left(\frac{\partial^2}{\partial x_1^2}-s^2\right)^2\widetilde{\Phi}^{(i)}=0, \tag{69}$$

$$\left(\frac{\partial^2}{\partial x_1^2}-s^2\right)\left[c^2\left(\frac{\partial^2}{\partial x_1^2}-s^2\right)-1\right]\widetilde{\varphi}_3^{(i)}=0, \tag{70}$$

$$\left[d^2\left(\frac{\partial^2}{\partial x_1^2}-s^2\right)-2\right]\widetilde{\varphi}_3^{(i)}=\left(\frac{\partial^2}{\partial x_1^2}-s^2\right)\widetilde{\Psi}_3^{(i)},\quad i=1,2. \tag{71}$$

Considering single-valuedness of the functions, the solution to the foregoing system is:

$$\widetilde{\Phi}^{(i)}=A^{(i)}e^{|s|x_1}+B^{(i)}x_1e^{|s|x_1}+C^{(i)}e^{-|s|x_1}+D^{(i)}x_1e^{-|s|x_1}, \tag{72}$$

$$\widetilde{\varphi}_3^{(i)}=E^{(i)}e^{|s|x_1}+F^{(i)}e^{\beta(s)x_1}+G^{(i)}e^{-|s|x_1}+H^{(i)}e^{-\beta(s)x_1}, \tag{73}$$

$$\widetilde{\Psi}_3^{(i)}=(d^2-2c^2)F^{(i)}e^{\beta(s)x_1}-\frac{E^{(i)}}{|s|}x_1e^{|s|x_1}+(d^2-2c^2)H^{(i)}e^{-\beta(s)x_1}+\frac{G^{(i)}}{|s|}x_1e^{-|s|x_1},$$
$$\text{for } i=1,2, \tag{74}$$

where $\beta(s) = \sqrt{s^2 + 1/c^2}$. The condition of vanishing response at infinity implies that $A^{(2)} = B^{(2)} = F^{(2)} = E^{(2)} = 0$. The remaining coefficients are to be determined from the transformed boundary conditions:

$$A_{\mathrm{s}}\left(-\imath s^3\widetilde{\Phi}^{(1)} + s^2\widetilde{\Psi}^{(1)}_{3,1}\right) + \mu\left(2\imath s\widetilde{\Phi}^{(1)}_{,1} - s^2\widetilde{\Psi}^{(1)}_{3} - \widetilde{\Psi}^{(1)}_{3,11}\right) - \alpha\left(\widetilde{\Psi}^{(1)}_{3,11} - s^2\widetilde{\Psi}^{(1)}_{3}\right) - 2\alpha\widetilde{\varphi}^{(1)}_{3}\Big|_{x_1=0} = 0, \tag{75}$$

$$-B_{\mathrm{s}}\left(s^4\widetilde{\Phi}^{(1)}_{,1} + \imath s^5\widetilde{\Psi}^{(1)}_{3}\right) + H_{\mathrm{s}}\left(-\imath s^3\widetilde{\varphi}^{(1)}_{3}\right) + (2\mu+\lambda)\left(\widetilde{\Phi}^{(1)}_{,11} - s^2\widetilde{\Phi}^{(1)}\right) + 2\mu\left(\imath s\widetilde{\Psi}^{(1)}_{3,1} + s^2\widetilde{\Phi}^{(1)}\right)\Big|_{x_1=0} = 0, \tag{76}$$

$$H_{\mathrm{s}}\left(-\imath s^2\widetilde{\varphi}^{(1)}_{3}\right) - 4L_{\mathrm{s}}\left(\widetilde{\varphi}^{(1)}_{3} + \imath s\widetilde{\Phi}^{(1)}_{,1} - s^2\widetilde{\Psi}^{(1)}_{3}\right) + (\gamma+e)\widetilde{\varphi}^{(1)}_{3,1}\Big|_{x_1=0} = 0, \tag{77}$$

$$\left(\imath s\widetilde{\Phi}^{(2)} - \widetilde{\Psi}^{(2)}_{3,1}\right) - \left(\imath s\widetilde{\Phi}^{(1)} - \widetilde{\Psi}^{(1)}_{3,1}\right)\Big|_{x_1=h} = \widetilde{F}(s), \tag{78}$$

$$\left(\widetilde{\Phi}^{(2)}_{,1} + \imath s\widetilde{\Psi}^{(2)}_{3}\right) - \left(\widetilde{\Phi}^{(1)}_{,1} + \imath s\widetilde{\Psi}^{(1)}_{3}\right)\Big|_{x_1=h} = 0, \tag{79}$$

$$\widetilde{\varphi}^{(2)}_{3} - \widetilde{\varphi}^{(1)}_{3}\Big|_{x_1=h} = 0, \tag{80}$$

$$(2\mu+\lambda)\left(\widetilde{\Phi}^{(2)}_{,11} - s^2\widetilde{\Phi}^{(2)}\right) + 2\mu\left(\imath s\widetilde{\Psi}^{(2)}_{3,1} + s^2\widetilde{\Phi}^{(2)}\right) - (2\mu+\lambda)\left(\widetilde{\Phi}^{(1)}_{,11} - s^2\widetilde{\Phi}^{(1)}\right) - 2\mu\left(\imath s\widetilde{\Psi}^{(1)}_{3,1} + s^2\widetilde{\Phi}^{(1)}\right)\Big|_{x_1=h} = 0, \tag{81}$$

$$\mu\left(2\imath s\widetilde{\Phi}^{(2)}_{,1} - s^2\widetilde{\Psi}^{(2)}_{3} - \widetilde{\Psi}^{(2)}_{3,11}\right) - \alpha\left(\widetilde{\Psi}^{(2)}_{3,11} - s^2\widetilde{\Psi}^{(2)}_{3}\right) - 2\alpha\widetilde{\varphi}^{(2)}_{3} - \mu\left(2\imath s\widetilde{\Phi}^{(1)}_{,1} - s^2\widetilde{\Psi}^{(1)}_{3} - \widetilde{\Psi}^{(1)}_{3,11}\right) + \alpha\left(\widetilde{\Psi}^{(1)}_{3,11} - s^2\widetilde{\Psi}^{(1)}_{3}\right) + 2\alpha\widetilde{\varphi}^{(1)}_{3}\Big|_{x_1=h} = 0 \tag{82}$$

$$\widetilde{\varphi}^{(2)}_{3,1} - \widetilde{\varphi}^{(1)}_{3,1}\Big|_{x_1=h} = 0, \tag{83}$$

and the transformed Cauchy–Riemann equations:

$$\widetilde{\Phi}^{(i)}_{,111} - s^2\widetilde{\Phi}^{(i)}_{,1} + \frac{2\mu\imath s}{(2\mu+\lambda)}\left[c^2\left(\widetilde{\varphi}^{(i)}_{3,11} - s^2\widetilde{\varphi}^{(i)}_{3}\right) - \widetilde{\varphi}^{(i)}_{3}\right] = 0, \tag{84}$$

$$\imath s\left(\widetilde{\Phi}^{(i)}_{,11} - s^2\widetilde{\Phi}^{(i)}\right) - \frac{2\mu}{(2\mu+\lambda)}\left[c^2\left(\widetilde{\varphi}^{(i)}_{3,111} - s^2\widetilde{\varphi}^{(i)}_{3,1}\right) - \widetilde{\varphi}^{(i)}_{3,1}\right] = 0, \tag{85}$$

for $i = 1, 2$. The latter equations enforce the compatibility condition on the problem and lead to three relations between the unknown coefficients:

$$G^{(1)} = \left(\frac{s}{\imath}\right)\left(\frac{2\mu+\lambda}{2\mu}\right)D^{(1)}, \tag{86}$$

$$G^{(2)} = \left(\frac{s}{\imath}\right)\left(\frac{2\mu+\lambda}{2\mu}\right)D^{(2)}, \tag{87}$$

$$E^{(1)} = \left(\frac{s}{\imath}\right)\left(\frac{2\mu+\lambda}{2\mu}\right)B^{(1)}. \tag{88}$$

We find the remaining nine coefficients using the nine boundary conditions presented above. The transformed functions $\widetilde{\Phi}^{(i)}$, $\widetilde{\varphi}^{(i)}_3$ and $\widetilde{\Psi}^{(i)}_3$ now allow us to determine the displacement and stress field components via their inverse transforms from (68) and the expressions (13)–(15). Thus, the complete analytical solution is given in terms of Fourier integrals.

4.1 Special case: reduction in classical elasticity

We set the micropolar elastic constants of the bulk material γ, e, and α as well as the micropolar surface rigidities H_{s} and L_{s} to zero. The coefficients $F^{(1)}$, $H^{(1)}$ and $H^{(2)}$, in turn, vanish. We normalize the system

of linear algebraic equations by taking $\widetilde{F}(s) = 1$ and calculate the remaining coefficients. The rest of the coefficients are determined as follows:

$$A^{(1)} = -\frac{\iota h(\mu+\lambda)\,|s|\,e^{-h|s|}}{2s(2\mu+\lambda)}, \tag{89}$$

$$B^{(1)} = -\frac{\iota\,|s|\,\mu e^{-h|s|}}{2s(2\mu+\lambda)}, \tag{90}$$

$$C^{(1)} = -\frac{C_1^{(1)}}{D}, \quad C^{(2)} = -\frac{C_1^{(2)}}{D}, \tag{91}$$

$$D^{(1)} = -\frac{D_1^{(1)}}{D}, \quad D^{(2)} = -\frac{D_1^{(2)}}{D}, \tag{92}$$

where

$$\begin{aligned} C_1^{(1)} =& \iota\,|s|\,s^2 e^{-h|s|}(\mu+\lambda)^2 \\ & \left\{\frac{2\mu(2\mu+\lambda)}{\mu+\lambda}\,|s|\left(h(B_{\mathrm{s}}s^2 - A_{\mathrm{s}}) + \frac{A_{\mathrm{s}}B_{\mathrm{s}}s^2}{\mu+\lambda}\right)\right. \\ & \left. + h\left(A_{\mathrm{s}}B_{\mathrm{s}}s^4 - 4\mu^2\right)\right\}, \end{aligned} \tag{93}$$

$$\begin{aligned} C_1^{(2)} =& \iota s^4 e^{-h|s|}(\mu+\lambda)^2 \left\{\left(\frac{4\mu^2}{|s|} + \frac{2\mu(2\mu+\lambda)}{\mu+\lambda}A_{\mathrm{s}}\right) h\left(e^{2h|s|}-1\right)\right. \\ & + A_{\mathrm{s}}B_{\mathrm{s}}s^2\,|s|\left(1 + \frac{3\mu+\lambda}{\mu+\lambda}e^{2h|s|}\right) \\ & \left. + s^2 B_{\mathrm{s}}\frac{2\mu(2\mu+\lambda)}{\mu+\lambda}\left(h\left(e^{2h|s|}+1\right) + \frac{A_{\mathrm{s}}}{\mu+\lambda}\right)\right\}, \end{aligned} \tag{94}$$

$$\begin{aligned} D_1^{(1)} =& \iota s^4 e^{-h|s|}\mu(\mu+\lambda)\left\{\left(\frac{1}{|s|} - 2h\right)\left(A_{\mathrm{s}}B_{\mathrm{s}}s^4 - 4\mu^2\right)\right. \\ & \left. - \frac{2\mu(2\mu+\lambda)}{\mu+\lambda}(B_{\mathrm{s}}s^2 - A_{\mathrm{s}})\right\}, \end{aligned} \tag{95}$$

$$\begin{aligned} D_1^{(2)} =& \iota s^4 e^{-h|s|}\mu(\mu+\lambda)\left\{\left(\frac{4\mu^2}{|s|} + \frac{2\mu(2\mu+\lambda)}{\mu+\lambda}s^2 B_{\mathrm{s}}\right)\left(e^{2h|s|}-1\right)\right. \\ & + A_{\mathrm{s}}B_{\mathrm{s}}s^2\,|s|\left(1 + \frac{3\mu+\lambda}{\mu+\lambda}e^{2h|s|}\right) \\ & \left. + \frac{2\mu(2\mu+\lambda)}{\mu+\lambda}A_{\mathrm{s}}\left(e^{2h|s|}+1\right) - 2A_{\mathrm{s}}B_{\mathrm{s}}hs^4 + 8\mu^2 h\right\}, \end{aligned} \tag{96}$$

$$\begin{aligned} D =& 2s^3\,|s|\,(2\mu+\lambda)(\mu+\lambda)\left\{\frac{4\mu^2}{|s|} + \frac{3\mu+\lambda}{\mu+\lambda}A_{\mathrm{s}}B_{\mathrm{s}}s^2\,|s|\right. \\ & \left. + \frac{2\mu(2\mu+\lambda)}{\mu+\lambda}\left(A_{\mathrm{s}} + 2B_{\mathrm{s}}s^2\right)\right\}. \end{aligned} \tag{97}$$

The stress components are obtained from the inverse integral transform:

$$\sigma_{\alpha\beta}^{(i)} = \frac{1}{\sqrt{2\pi}}\int_{-\infty}^{\infty}\widetilde{F}(s)\widetilde{\sigma}_{\alpha\beta}^{(i)}e^{\iota s x_2}\mathrm{d}x_2, \quad i = 1, 2,\ \alpha, \beta = 1, 2. \tag{98}$$

where $\widetilde{F}(s)$ is the Fourier transform of $bH(-x_2)$ and

$$\widetilde{\sigma}_{11}^{(i)} = (2\mu+\lambda)\left(\widetilde{\Phi}_{,11}^{(i)} - s^2\widetilde{\Phi}^{(i)}\right) + 2\mu\left(\imath s\widetilde{\Psi}_{3,1}^{(i)} + s^2\widetilde{\Phi}^{(i)}\right), \tag{99}$$

$$\widetilde{\sigma}_{22}^{(i)} = (2\mu+\lambda)\left(\widetilde{\Phi}_{,11}^{(i)} - s^2\widetilde{\Phi}^{(i)}\right) - 2\mu\left(\imath s\widetilde{\Psi}_{3,1}^{(i)} + \widetilde{\Phi}_{,11}^{(i)}\right), \tag{100}$$

$$\widetilde{\sigma}_{12}^{(i)} = \widetilde{\sigma}_{21}^{(i)} = \mu\left(2\imath s\widetilde{\Phi}_{,1}^{(i)} - s^2\widetilde{\Psi}_{3}^{(i)} - \widetilde{\Psi}_{3,11}^{(i)}\right), \quad i = 1, 2. \tag{101}$$

It is not difficult to see that on removing the flexural rigidity of the surface we recover the results presented by Intarit et al. [38].

5 Numerical examples

We determine the constants from the system of algebraic equations and hence the transformed functions $\widetilde{\Phi}^{(i)}$, $\widetilde{\Psi}_3^{(i)}$, and $\widetilde{\varphi}_3^{(i)}$. We use these functions and the corresponding inverse integral transforms of the stress components to acquire the complete solution. The solution of the stress field components in the form of improper integrals is then computed using numerical integration methods. In order to compare our results with those in the existing literature, we adopt classical elastic constants equivalent to those of an aluminum alloy with surface parameters for an Al[1,1,1] type surface. Additionally, we consider hypothetical values for bending rigidity for the surface as well as for the micropolar properties. For the purpose of comparison, we define a surface characteristic length, $l_{\mathrm{s}} = A_{\mathrm{s}}(2\mu+\lambda)/2\mu(\mu+\lambda)$ as in [38]. Accordingly, the numerical values for the most general case are taken as:

$$\mu = 26.1\,\mathrm{GPa}, \quad \lambda = 58.1\,\mathrm{GPa}, \quad \alpha = 2.6\,\mathrm{GPa}, \quad \gamma = 2.6\,\mathrm{GPa},$$
$$A_{\mathrm{s}} = 6.091\,\mathrm{N/m}, \quad B_{\mathrm{s}} = 0.024\,\mathrm{N\,m}, \quad H_{\mathrm{s}} = 0.024\,\mathrm{N\,m}, \quad L_{\mathrm{s}} = 0.953\,\mathrm{N}.$$

Again we note that the above values are chosen for illustrative purposes only and to demonstrate the effects of each parameter on the solution. In this area of study, it is almost always the case that the theory is ahead of the experiments making the availability of real parametric data almost impossible to find. We normalize the dimensions in our analysis by the characteristic length of the surface l_{s}. Therefore, we set the normalized measure of depth of the dislocation to $\overline{h} = h/l_{\mathrm{s}}$, and the normalized coordinates to $\overline{x}_1 = x_1/l_{\mathrm{s}}$ and $\overline{x}_2 = x_2/l_{\mathrm{s}}$. We illustrate the stress components σ_{11}, σ_{12}, and σ_{22} at two different relative depths along the x_2 direction: $\overline{x}_1 = 0.1$ and $\overline{x}_1 = 1$. We compare five different material models to observe the changes in the solution. The solutions corresponding to classical elastic materials without and with G–M surface effects are published in [38]. Here they are obtained as special cases of our results by letting the micropolar and extra surface parameters B_{s}, H_{s}, L_{s}, α, and γ, be set to zero. We introduce three additional cases: a micropolar material without surface effects ($A_{\mathrm{s}} = B_{\mathrm{s}} = H_{\mathrm{s}} = L_{\mathrm{s}} = 0$); a classical material with higher-order surface effects ($\alpha = \gamma = H_{\mathrm{s}} = L_{\mathrm{s}} = 0$); and the most general case of a micropolar material with higher-order surface effects incorporating both bending and twisting rigidities.

Figure 3 shows the distribution of the normal stress component σ_{11} along the x_2 direction at the depths $\overline{x}_1 = 0.1$ and $\overline{x}_1 = 1$ induced by an edge dislocation at the depth $\overline{h} = 1$. Looking at the stress profile at the relative depth 0.1, we observe that the use of classical and micropolar theories in the absence of surface elasticity intensifies σ_{11} at this depth only slightly, while involving surface flexural and micropolar effects for both classical and micropolar theories significantly affects the solution. The classical G–T model yields higher stress values compared to the absence of surface effects, but lower values compared to the classical and micropolar flexural effects of the surface. Interestingly, the stress distributions for the classical and micropolar surface flexural effects are close to each other. On the other hand, at the relative depth $\overline{x}_1 = 1$, the normal stress component σ_{11} decreases by considerations of micropolarity and surface effects of all kind. The differences are more pronounced especially near the dislocation core. Among the surface models, the micropolar surface involving all the rigidity aspects presents the lowest intensity of stress distribution along the slip plane, $\overline{x}_1 = 1$, near the dislocation core.

Figure 4 shows the distribution of shearing component σ_{12} at two different relative depths, $\overline{x}_1 = 0.1$ and $\overline{x}_1 = 1$. We observe that including micropolar effects of the bulk into the problem decreases the shear stress intensity on the plane $\overline{x}_1 = 0.1$. However, farther away from the dislocation core, the solutions of classical and micropolar elasticity converge. In this case, the classical G–M surface elasticity intensifies the stress, while

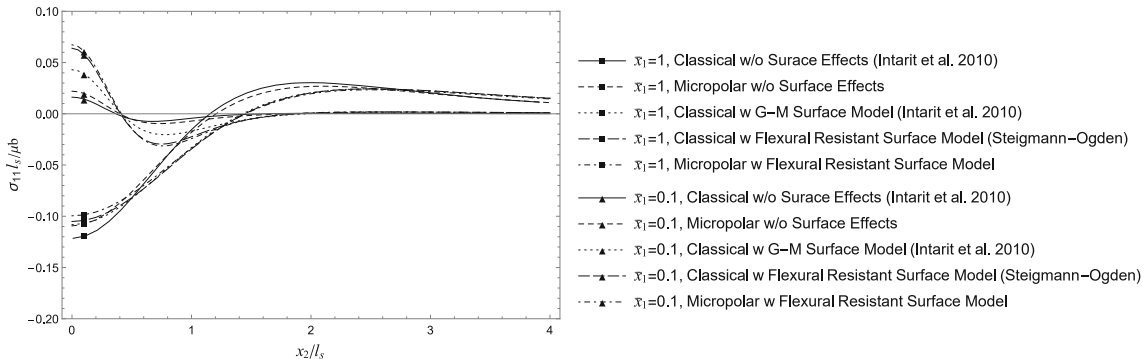

Fig. 3 Variation of the normalized stress component σ_{11} at relative depths $\overline{x}_1 = 0.1$ and $\overline{x}_1 = 1$, for an edge dislocation at $\overline{h} = 1$

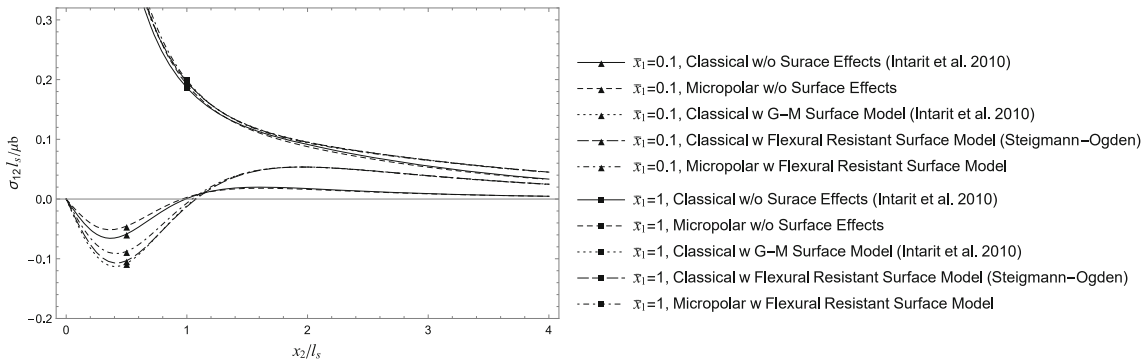

Fig. 4 Variations of the normalized stress component σ_{12} at relative depths $\overline{x}_1 = 0.1$ and $\overline{x}_1 = 1$, for an edge dislocation at $\overline{h} = 1$

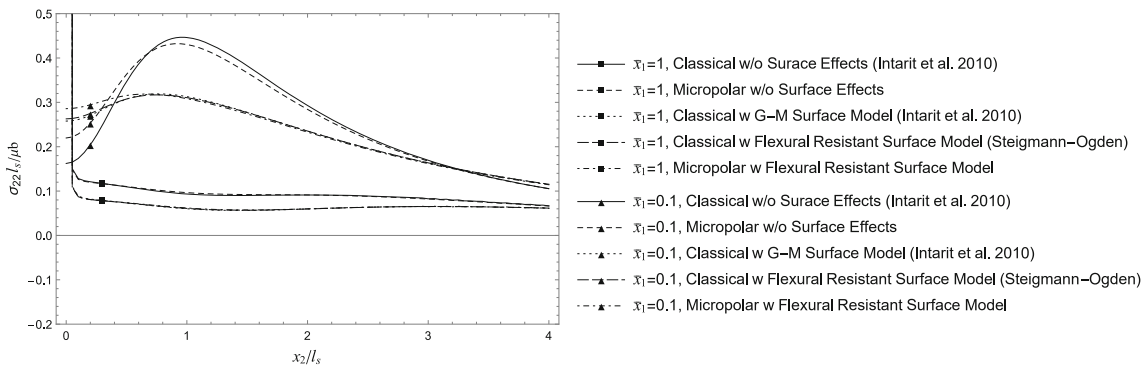

Fig. 5 Variations of the normalized stress component σ_{22} at relative depths $\overline{x}_1 = 0.1$ and $\overline{x}_1 = 1$, for an edge dislocation at $\overline{h} = 1$

incorporating micropolar and flexural effects of the surface lowers the results. The classical bending rigidity of the surface has a marginal effect on the stress component, σ_{12}, at this depth. For the shear stress distribution at the slip plane, we notice the singularity at the dislocation core for all cases. However, involving micropolarity of the bulk and surfaces effects with various properties intensify the singularity rate of the solution. The most extreme case happens for the most general case of a micropolar material with the flexural resistant surface. It is interesting that the micropolar properties of the bulk affect the stress distribution locally near the dislocation core, while all types of surface effects alter the stress distributions even at far away distances from the dislocation core. This is true for the other components of stress as well.

Figure 5 shows the distribution profile of the normal stress component σ_{22}. We observe that the incorporation of surface elasticity reduces the stress variation range at the depth $\overline{x}_1 = 0.1$. However, the stress intensity increases near the core by adopting surface effects of any kind. The incorporation of classical bending rigidity in the surface makes an insignificant contribution to the solution compared to analogous results using the regular

G–M model. The micropolar surface with bending and twisting rigidities, however, has a higher influence on the profile of the stress component, σ_{22}. At the depth $\overline{x}_1 = 1$, we simply observe that the classical bending rigidity and micropolar effects of the surface do not affect the stress profile. In addition, the micropolarity of the material without surface effects makes no contribution to the stress profile at this depth. For both illustrated depths in Fig. 5 and also Figs. 3 and 4, we observe that the surface effects cause a global change in the pattern of the stress distribution. Different types of surfaces affect the solution at a certain distance from the dislocation core; however, the type of surface model in use becomes less important at distances far from the dislocation core. The same conclusion can be reached when surface effects are ignored altogether in classical and micropolar formulations. Consequently, at relatively far away distances from the dislocation core, we have two distinct responses: one arising from the inclusion of surface effects (relatively independent of the surface model used) and one which does not include surface effects irrespective of the type of surface or bulk elasticity model used.

6 Conclusion

We have formulated a micropolar elastic surface model incorporating classical bending and micropolar twisting rigidities for plane strain deformations. The corresponding boundary value problem reduces to a system of second-order elliptic partial differential equations with boundary conditions of the fourth order. We used the surface model to solve a fundamental problem of an edge dislocation close to the surface of a half-plane. By solving this problem, we demonstrated that the proposed model can indeed be successfully applied to fundamental problems of plane elasticity. We conclude that the classical G–M surface model may not be sufficient for materials in which micropolar bulk effects and surface twisting rigidities are significant. Additionally, despite the fact that classical bending resistance of the surface may alter the solution only marginally, the incorporation of this surface effect in the model of deformation may still prove to be useful in certain cases, for example, in the presence of a reinforcement attached to the boundary of the solid. Finally, we conclude that for the stress components in the dislocation problem studied here, the particular choice of surface and bulk elasticity models is important relatively close to the dislocation core. However, farther away from the dislocation core only the incorporation of surface effects (of any type) significantly affects the solution.

Acknowledgements Schiavone thanks the Natural Sciences and Engineering Research Council of Canada for its support through a Discovery Grant (Grant No: RGPIN – 2017 - 03716115112).

References

1. Li, S., Wang, G.: Introduction to Micromechanics and Nanomechanics. World Scientific, Singapore (2008)
2. Eringen, A.C.: Simple microfluids. Int. J. Eng. Sci. **2**(2), 205–217 (1964)
3. Eringen, A.C., Suhubi, E.S.: Nonlinear theory of simple micro-elastic solids—I. Int. J. Eng. Sci. **2**(2), 189–203 (1964)
4. Suhubl, E.S., Eringen, A.C.: Nonlinear theory of micro-elastic solids—II. Int. J. Eng. Sci. **2**(4), 389–404 (1964)
5. Eringen, A.C.: Continuum Physics. Volume—Polar and Nonlocal Field Theories. Academic Press, New York (1976)
6. Eringen, A.C.: Linear theory of micropolar elasticity. J. Math. Mech. **15**(6), 909–923 (1966)
7. Wang, X., Lee, J.D.: Micromorphic theory: a gateway to nano world. Int. J. Smart Nano Mater. **1**(2), 115–135 (2010)
8. Kaloni, P.N., Ariman, T.: Stress concentration effects in micropolar elasticity. Acta Mech. **4**(3), 216–229 (1967)
9. Warren, W.E., Byskov, E.: A general solution to some plane problems of micropolar elasticity. Eur. J. Mech. A. Solids **27**, 18–27 (2008)
10. Eringen, A.C.: Theory of micropolar plates. ZAMP **18**(1), 12–30 (1967)
11. Eremeyev, V.A., Lebedev, L.P., Altenbach, H.: Foundations of Micropolar Mechanics. Springer, Berlin (2013)
12. Sharma, P., Dasgupta, A.: Average elastic fields and scale-dependent overall properties of heterogeneous micropolar materials containing spherical and cylindrical inhomogeneities. Phys. Rev. B **66**(224110), 1–10 (2002)
13. Gurtin, M.E., Murdoch, A.I.: A continuum theory of elastic material surfaces. Arch. Ration. Mech. Anal. **57**, 291–323 (1975)
14. Gurtin, M.E., Murdoch, A.I.: Surface stress in solids. Int. J. Solids Struct. **14**(6), 431–440 (1978)
15. Sharma, P., Ganti, S., Bhate, N.: Effect of surfaces on the size-dependent elastic state of nano-inhomogeneities. Appl. Phys. Lett. **82**, 535–537 (2003)
16. Tian, L., Rajapakse, R.K.N.D.: Analytical solution for size-dependent elastic field of a nanoscale circular inhomogeneity. J. Appl. Mech. **74**(3), 568–574 (2007)
17. Miller, R.E., Shenoy, V.B.: Size-dependent elastic properties of nanosized structural elements. Nanotechnology **11**, 139–147 (2000)
18. Duan, H.L., Wang, J., Huang, Z.P., Karihaloo, B.L.: Size-dependent effective elastic constants of solids containing nano-inhomogeneities with interface stress. J. Mech. Phys. Solids **53**(7), 1574–1596 (2005)

19. Mogilevskaya, S., Crouch, S., La Grotta, A., Stolarski, H.: The effects of surface elasticity and surface tension on the transverse overall elastic behavior of unidirectional nano-composites. Compos. Sci. Technol. **70**(3), 427–434 (2010)
20. Steigmann, D.J., Ogden, R.W.: Plane deformations of elastic solids with intrinsic boundary elasticity. Proc. R. Soc. A **453**(1959), 853–877 (1997)
21. Steigmann, D.J., Ogden, R.W.: Elastic surface-substrate interactions. Proc. R. Soc. A **455**(1982), 437–474 (1999)
22. Andreussi, F., Gurtin, M.E.: On the wrinkling of a free surface. J. Appl. Phys. **48**(9), 3798–3799 (1977)
23. Schiavone, P., Ru, C.Q.: Integral equation methods in plane-strain elasticity with boundary reinforcement. Proc. R. Soc. A **454**, 2223–2242 (1998)
24. Schiavone, P., Ru, C.Q.: The traction problem in a theory of plane strain elasticity with boundary reinforcement. Math. Mech. Solids **5**(1), 101–115 (2000)
25. Chhapadia, P., Mohammadi, P., Sharma, P.: Curvature-dependent surface energy and implications for nanostructures. J. Mech. Phys. Solids **59**(10), 2103–2115 (2011)
26. Chen, T., Chiu, M.S.: Effects of higher-order interface stresses on the elastic states of two-dimensional composites. Mech. Mater. **43**(4), 212–221 (2011)
27. Benveniste, Y., Miloh, T.: Imperfect soft and stiff interfaces in two-dimensional elasticity. Mech. Mater. **33**(6), 309–323 (2001)
28. Eremeyev, V.A., Lebedev, L.P.: Mathematical study of boundary-value problems within the framework of Steigmann–Ogden model of surface elasticity. Contin. Mech. Thermodyn. **28**(1–2), 407–422 (2016)
29. Dai, M., Gharahi, A., Schiavone, P.: Analytic solution for a circular nano-inhomogeneity with interface stretching and bending resistance in plane strain deformations. Appl. Math. Modell. **55**, 160–170 (2018)
30. Zemlyanova, A.Y., Mogilevskaya, S.G.: Circular inhomogeneity with steigmann-ogden interface: local fields, neutrality, and maxwell's type approximation formula. Int. J. Solids Struct. **135**, 85–98 (2018)
31. Zemlyanova, A.Y.: Frictionless contact of a rigid stamp with a semi-plane in the presence of surface elasticity in the Steigmann–Ogden form. Math. Mech. Solids **23**(8), 1140–1155 (2018)
32. Zemlyanova, A.Y.: A straight mixed mode fracture with the Steigmann–Ogden boundary condition. Q. J. Mech. Appl. Math. **70**(1), 65–86 (2017)
33. Zemlyanova, A.Y.: The effect of a curvature-dependent surface tension on the singularities at the tips of a straight interface crack. Q. J. Mech. Appl. Math. **66**(2), 199–219 (2013)
34. Chen, H., Hu, G., Huang, Z.: Effective moduli for micropolar composite with interface effect. Int. J. Solids Struct. **44**(25–26), 8106–8118 (2007)
35. Sigaeva, T., Schiavone, P.: Surface effects in anti-plane deformations of a micropolar elastic solid: integral equation methods. Contin. Mech. Thermodyn. **28**(1), 105–118 (2016)
36. Sigaeva, T., Schiavone, P.: Influence of boundary elasticity on a couple stress elastic solid with a mode-III crack. Quart. J. Mech. Appl. Math. **68**(2), 195–202 (2015)
37. Gharahi, A., Schiavone, P.: Plane micropolar elasticity with surface flexural resistance. Contin. Mech. Thermodyn. **30**(3), 675–688 (2018)
38. Intarit, P., Senjuntichai, T., Rajapakse, R.K.N.D.: Dislocations and internal loading in a semi-infinite elastic medium with surface stresses. Eng. Fract. Mech. **77**(18), 3592–3603 (2010). (Computational mechanics in fracture and damage: a special issue in Honor of Prof. Gross)
39. Nowacki, W.: Theory of Asymmetric Elasticity. Pergamon Press, Oxford (1986)